Dalton Transactions

PAPER

Cite this: *Dalton Trans.*, 2019, **48**, 15849

Acetylenedicarboxylate-based cerium(IV) metal–organic framework with fcu topology: a potential material for air cleaning from toxic halogen vapors†

Tobie J. Matemb Ma Ntep,[a] Helge Reinsch,[b] Jun Liang[a,c] and Christoph Janiak *[a]

Received 30th August 2019,
Accepted 1st October 2019

DOI: 10.1039/c9dt03518d

rsc.li/dalton

The most contracted cerium(IV)-based metal–organic framework (MOF) with **fcu** topology incorporating an alkyne-based linker, namely acetylenedicarboxylate (ADC), was synthesized under green conditions in water at room temperature and thoroughly characterized. The structure of this new MOF, denoted as Ce-HHU-1, was determined from powder X-ray diffraction data and Rietveld refinement and is made up of octahedral $[Ce_6O_4(OH)_4]^{12+}$ clusters, each of which is connected to other inorganic units by twelve ADC linkers to give a porous network with **fcu** topology analogous with UiO-66. The permanent microporosity of Ce-HHU-1 was confirmed by nitrogen sorption, meanwhile its high hydrophilicity was displayed by a type I water vapor sorption isotherm. The adsorption of CO_2 in Ce-HHU-1 features a remarkably high zero-coverage isosteric heat of adsorption of 47 kJ mol^{-1}, attributed to the presence of the –C≡C– triple-bond in the framework. The latter also allows for Ce-HHU-1 to capture and irreversibly chemisorb Br_2 vapors, as well as both chemi- and physisorb I_2 vapors in an effective manner, making this material potentially applicable for air cleaning from toxic halogen vapors.

Introduction

Metal–organic frameworks (MOFs) based on cerium(IV) (Ce(IV)-MOFs) have recently attracted scientific attention due to the redox activity of Ce(IV), yielding MOFs applicable in redox-catalysis,[1] and photocatalysis.[2] Constructed by connecting Ce-oxido clusters by organic ligands into porous materials, Ce-MOFs are usually obtained by easy synthetic route within few minutes. Since the first report in 2015 by Lammert *et al.* of conditions to stabilize Ce(IV) cations in a MOF,[3] many Ce-MOFs have been synthesized displaying various net topologies including **reo**, **spn**, **scu**, **she**, **scq** and **fcu**, depending on the employed linker geometry.[4,5] However, Ce-MOFs with the **fcu** topology like UiO-66 are by far the most representative.[6] Their structure consists of octahedral $[Ce_6O_4(OH)_4]^{12+}$ secondary building units (SBUs), which are twelvefold connected to other units by linear dicarboxylate linkers, forming an expanded cubic close-packed porous framework.[7] In this regard, many linear dicarboxylate linkers have been used including benzene-1,4-dicarboxylate, fumarate, 2,2′-bipyridine-5,5′-dicarboxylate, pyridine-2,5-dicarboxylate, naphthalene-2,6-dicarboxylate, biphenyl-4.4′-dicarboxylate.[3,4] However, no Ce-MOF based on acetylenedicarboxylate (ADC) as the shortest straight linear alkyne-based dicarboxylate linker (Scheme 1) is yet reported.

Very few ADC-based MOFs are known. Serre *et al.* obtained the first Eu(III)-acetylenedicarboxylate open framework, which showed irreversible pore contraction upon pore evacuation by dehydration.[8] Tranchemontagne *et al.* synthesized Zn-acetylenedicarboxylate, the smallest member of IRMOF series

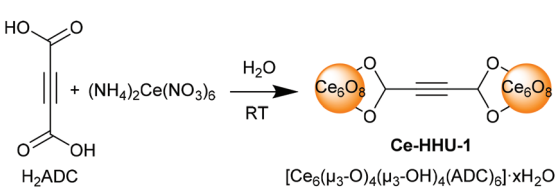

Scheme 1 Reaction of acetylenedicarboxylic acid to the UiO-type MOF Ce-HHU-1.

[a]*Institut für Anorganische Chemie und Strukturchemie, Heinrich-Heine-Universität Düsseldorf, Universitätsstraße 1, D-40225 Düsseldorf, Germany. E-mail: janiak@hhu.de*
[b]*Institut für Anorganische Chemie, Christian-Albrechts-Universität zu Kiel, Max-Eyth-Straße 2, 24118 Kiel, Germany*
[c]*Hoffmann Institute of Advanced Materials, Shenzhen Polytechnic, 7098 Liuxian Blvd, Nanshan District, Shenzhen 518055, China*

†Electronic supplementary information (ESI) available: Additional information on PXRD, IR, Raman, TGA, Rietveld refinement, halogen adsorption, isosteric heat of CO_2 adsorption. CCDC 1946853. For ESI and crystallographic data in CIF or other electronic format see DOI: 10.1039/c9dt03518d

(IRMOF-0), albeit as non-porous material due to double-interpenetration and trapped guest solvent molecules that could not be removed.[9] Gramm *et al.* also synthesized a series of three-dimensional rare-earth acetylenedicarboxylate-based coordination polymers,[10] so extending a previous work of Michaelides *et al.*[11] However, none of these works could prove the permanent porosity of the obtained ADC-based coordination polymers. Obviously, despite its simplicity as linear linker, obtaining acetylenedicarboxylate-based metal–organic frameworks with experimentally proven permanent porosity had been a challenge in the MOF field. Nevertheless, we recently reported the synthesis and porosity studies of an acetylenedicarboxylate-based zirconium-MOF having the **fcu** topology, namely Zr-HHU-1 (HHU stands for Heinrich-Heine-University Düsseldorf). This work was the first report of an ADC-based MOF presenting experimentally assessed permanent porosity.[12]

Employing the ADC linker in the construction of MOFs is of great interest not only because it provides MOFs spaced solely by linear carbon arrays (hydrogen-free linker) but also because of the functionalizable –C≡C– triple-bond (Scheme 1). We demonstrated that this could involve an *in situ* hydrohalogenation to halogen functionalized MOFs.[12] In addition, the alkyne function could be the basis for post-synthetic modification of the constructed ADC-based MOF *via* addition reactions. Post-synthetic halogenation of integral unsaturated C–C bonds are known for Zr- and Hf-MOFs constructed from 4,4′-ethynylene-dibenzoate and 4,4′-(buta-1,3-diyne-1,4-diyl)-dibenzoate linkers.[13] Furthermore, the presence of –C≡C– triple bonds in the porous material could enhance the adsorption affinity/capacity of some gases like CO_2, as well as vapors like water and molecular halogens.[12,14]

To broaden the scope of porous acetylenedicarboxylate-based MOFs containing M(IV) cations, we herein report the synthesis, structural characterization, porosity and gas/vapor sorption properties of a new **fcu** Ce(IV)-MOF based on the simple ADC linker (Scheme 1). We also investigate the adsorption of bromine and iodine vapors in the new material, in view of its application for air cleaning from these toxic halogen vapors.

Experimental

Materials and methods

Cerium(IV) ammonium nitrate [$(NH_4)_2Ce(NO_3)_6$, purity 99%] was obtained from Acros Organics; acetylenedicarboxylic acid (H_2ADC, purity 97%) was obtained from abcr; bromine (Br_2, technical grade) from Merck Schuchardt OHG, and iodine (I_2, purity 99.5%) from Grüssing.

Powder X-ray diffraction (PXRD) patterns were recorded with the Brucker D2 Phaser diffractometer using a Cu-Kα1/α2 radiation with λ = 1.5418 Å at 30 kV. Diffractograms were obtained on a flat silicon layer sample holder, with 2θ angles ranging within 5–50° at a scan rate of 0.0125° s^{-1}.

The **infrared (IR)** spectrum was obtained on a Bruker FT-IR Tensor 37 Spectrometer in the 4000–550 cm^{-1} region with 2 cm^{-1} resolution as KBr disk. The **Raman** spectra were measured on a Bruker MultiRAM-FT Raman spectrometer equipped with a Nd:YAG-laser (wavelength 1064 nm).

Scanning electron microscopy (SEM) images were obtained using a Jeol JSM-6510LV QSEM advanced electron microscope with a LaB_6 cathode at 5–20 keV. The samples for SEM imaging were coated with gold using a Jeol JFC 1200 fine-coater (20 mA for 25 s).

Thermogravimetric analysis (TGA) was carried out on a Netzsch TG209 F3 Tarsus device under synthetic air atmosphere and heating at a ramp rate of 5 K min^{-1} to 600 °C.

Liquid ^{13}C NMR spectra were measured with a Bruker Avance III-300 (300 MHz). Prior to solution NMR analysis, 20 mg of Ce-HHU-1-Br_2 were dissolved in 0.5 mL of DMSO-d_6. For Ce-HHU-1-I_2, 20 mg of iodine-desorbed MOF were suspended in DMSO-d_6 (0.65 mL) and 5 drops of DCl (35 wt% in D_2O) were added. After about 1 h, the yellowish formed solution was introduced in the NMR tube for the analysis.

Nitrogen and CO_2 sorption isotherms were measured with a Micromeritics ASAP 2020 automatic gas sorption analyzer at 77 K (N_2), 273 K and 293 K (CO_2). The Brunauer–Emmett–Teller (BET) specific surface area and pore volume were evaluated from the nitrogen physisorption isotherms.

Water sorption isotherm was obtained using a VSTAR™ vapor sorption analyzer from Quantachrome.

Water-based synthesis of Ce-HHU-1 at ambient temperature

In a 25 mL glass vial, 364 mg (3.2 mmol) of acetylenedicarboxlic acid were dissolved in 12 mL of water. 2 mL of an aqueous solution of cerium ammonium nitrate (0.533 M) was added under stirring. The yellowish precipitate, which was formed instantly under mixture of the two solutions, was stirred for 15 min and separated from the mother liquor by centrifugation. The solid product was then washed twice with water and twice with ethanol and then centrifuged.

The activated sample was obtained by supercritical CO_2 ($scCO_2$) drying of the as-synthesized material, followed by outgassing under dynamic vacuum for 16 h at 40 °C. The use of supercritical CO_2 drying as activation procedure was adopted because of the low thermal stability of Ce-HHU-1 (stable only until about 120 °C, from TGA, Fig. S4, ESI†). We experienced in our previous works that the analogous frameworks of Zr-HHU-1 and Hf-HHU-1 collapse over conventional activation by heating at temperatures above 100 °C under vacuum.[12] Since the acetylenedicarboxylate linker is thermally labile, the supercritical CO_2 drying enables to avoid high temperatures for de-solvating/outgassing the pores of Ce-HHU-1. Elemental analysis of the activated sample: calcd for $Ce_6C_{24}H_4O_{32}$ = $[Ce_6O_4(OH)_4(OOC\text{-}C{\equiv}C\text{-}COO)_6]$: C 17.52%, H 0.24%; found: C 18.33%, H 1.09%. Yield: 270 mg (92%) based on the cerium salt.

Bromine adsorption

30 mg of activated Ce-HHU-1 were distributed in a small open vial, and a small amount of bromine was introduced in another open vial (see Fig. 7). The two vials were transferred in a vessel that was sealed to ensure a closed system. The sealed vessel was allowed to stand at room temperature over a week.

Iodine adsorption

About 40 mg of activated sample of Ce-HHU-1 were distributed in a small open vial, while about 100 mg I_2 crystals were distributed in a second open vial. The two vials were transferred together in a vessel that was sealed to ensure a closed system and stored at room temperature (see Fig. S9 in ESI†). Iodine uptake was measured gravimetrically after regular adsorption times.

Results and discussion

Synthesis and characterization

The new acetylenedicarboxylate-based cerium(IV)–metal–organic framework termed as Ce-HHU-1 of formula $[Ce_6(\mu_3\text{-}O)_4(\mu_3\text{-}OH)_4(ADC)_6]\cdot xH_2O$, was quantitatively obtained immediately after mixing aqueous solutions of acetylenedicarboxylic acid and cerium(IV) ammonium nitrate (Scheme 1). It should be noted that early syntheses of Ce(IV)-MOFs were performed in a DMF/water solvent mixture with at times addition of a monocarboxylic acid modulator like acetic or formic acid. In the case of Ce-HHU-1, the synthesis is carried out in water only and requires neither organic solvents like DMF, nor monocarboxylic acid modulator. Furthermore, although a water-based synthesis of Ce(IV)-MOF was recently reported at about 100–110 °C,[15] our synthesis takes place at room temperature and within a shorter reaction time, making the synthesis of Ce-HHU-1 even greener, as it consumes no energy from heating. This easy synthesis would also enable to produce Ce-HHU-1 at a large scale and competitive cost. This aspect is very important considering industrial production of this material towards commercial applications. The production of metal–organic frameworks in a clean, fast and economical way is a current challenge to take MOFs from laboratories to industries towards practical applications.[16]

Interestingly, Ce-HHU-1 displays a very high crystallinity in spite of its very rapid formation. SEM images of Ce-HHU-1 (Fig. S15, ESI†) reveal that the obtained product is made of agglomerated crystallites. Individual crystals have a size of about 100 nm, with no specific shape. The PXRD pattern of the obtained yellow microcrystalline powder of Ce-HHU-1 resembles that of zirconium acetylenedicarboxylate (Zr-HHU-1) (Fig. 1 and Fig. S1 in ESI†). However, the reflections in Ce-HHU-1 are slightly shifted to lower values compared to those of Zr-HHU-1. This indicates that the two MOFs are analogues, with Ce-HHU-1 having a slightly larger cell parameter, which is consistent with a larger ionic radius of Ce^{4+} (0.97 Å) in comparison to Zr^{4+} (0.84 Å).[17]

The strong band in the Raman spectrum at 2225 cm^{-1} (Fig. S2 in ESI†) is ascribed to the stretching vibration of the –C≡C– triple-bond of the ADC linker. The bands at 1600 cm^{-1} and 1371 cm^{-1} in the infrared spectrum (Fig. S3 in ESI†) are due to asymmetric and symmetric vibrations of coordinated carboxylate of the linker respectively.

The thermogravimetric analysis (Fig. S4, ESI†) shows that Ce-HHU-1 is thermally stable to about 120 °C. After this temperature, the material is decomposed in two steps to yield a solid residue that was identified by PXRD to be CeO_2 (see PXRD of residue in Fig. S5, ESI†). Ce-HHU-1 is thermally less stable than Zr-HHU-1 (180 °C).[12] This is expected, as UiO-type Ce(IV)-MOFs feature lower thermal stability compared to their zirconium analogues.[3] Furthermore, the vast majority of ADC-based coordination polymers/complexes feature low thermal stability (<250 °C) with some even decomposing in air at room temperature.[18] An exception is that of Sr-ADC for which a thermal stability of up to 440 °C was observed.[19] This relatively low thermal stability is attributable to the thermal liability of H_2ADC linker. Solid acetylenedicarboxylic acid decomposes at 180 °C. However, Ce-HHU-1 has a good hydrolytic and chemical stability, as it maintains its crystallinity after stirring in water, acidic solution (pH = 1) and various solvents at room temperature for 24 h (Fig. S6 and S7, ESI†). Unfortunately, Ce-HHU-1 would degrade in an alkaline solution (pH = 12) under the same treatment.

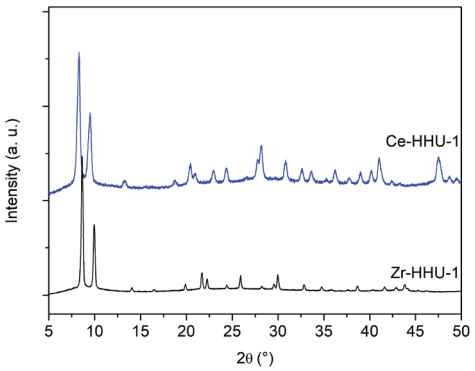

Fig. 1 Powder X-ray diffractogram of Ce-HHU-1 compared to Zr-HHU-1. The patterns are similar with that of Ce-HHU-1 being slightly shifted to lower 2θ angle values.

The analysis of the TG curve reveals that the obtained Ce-HHU-1 contains no missing linker defects. This result is in accordance with other reports of Ce(IV)-MOFs synthesized without monocarboxylic acid modulator.[4] Missing ligand defective sites in UiO-type Zr-MOFs are mainly due to the use of monocarboxylic acid modulators. Indeed, a defect free UiO-66 MOF was obtained by Lillerud *et al.* from a synthesis done without monocarboxylic acid modulator.[20]

Structure

The structure of Ce-HHU-1 was determined by means of Rietveld refinement from powder diffraction data obtained in transmission geometry on a STOE Stadi MP, equipped with a Dectris Mythen detector and using monochromated CuKα1 radiation. The indexation was done using TOPAS academics[21] (details in ESI†). Some relevant parameters are summarized in Table 1 and the final plot is shown in Fig. 2. Crystallographic data for the structure of Ce-HHU-1 have been deposited with the Cambridge Crystallographic Data Center (CCDC 1946853†).

The structure of Ce-HHU-1 consists of a face centered cubic **fcu** net topology in space group $Fm\bar{3}m$ like UiO-66.[7] Its frame-

Table 1 Selected parameters for the Rietveld refinement of Hf-HHU-1

Compound	Ce-HHU-1
Crystal system	Cubic
Space group	$Fm\bar{3}m$
$a = b = c$/Å	19.1733(6)
$\alpha = \beta = \gamma$/°	90
V/Å^3	7048.4(6)
R_{wp}/%	6.6
R_{Bragg}/%	3.0
GoF	2.1

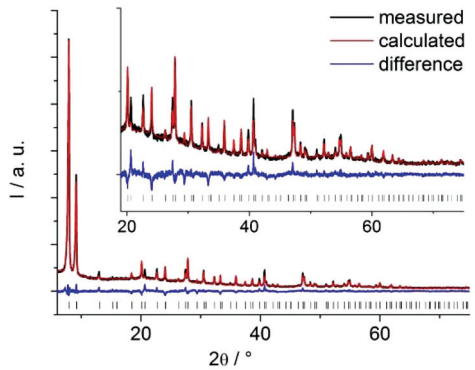

Fig. 2 Final Rietveld plot for Ce-HHU-1. The black curve represents the measured data, the red curve is the theoretical data and the blue curve indicates the difference. Vertical black bars mark the allowed Bragg reflection positions.

work is built up of octahedral $[Ce_6(\mu_3\text{-}O)_4(\mu_3\text{-}OH)_4]$ SBUs each connected to other units by twelve ADC linkers. This results in a porous network having tetrahedral cages of 5.8 Å diameter and octahedral cages of 9.6 Å diameter. Pores are accessible through triangular windows of about 4 Å diameter (Fig. 3). Ce-HHU-1 can therefore be regarded as the most contracted **fcu** Ce(IV)-MOF incorporating an alkyne-based linker, that is a framework of –C≡C– triple bonds joined at Ce_6O_8 SBUs.

Porosity, water vapor and CO_2 adsorption

The porosity of Ce-HHU-1 was assessed by nitrogen sorption experiment conducted with an activated (solvent evacuated) sample at 77 K. The obtained isotherm is of type I (Fig. 4), corresponding to a permanently microporous material.[22] The calculated BET surface area and micropore volume amount to 793 m^2 g^{-1} and 0.24 cm^3 g^{-1} respectively. These values are comparable with the BET surface area and micropore volume previously reported for cerium(IV) fumarate Ce-UiO-66-Fum (S_{BET} = 732 m^2 g^{-1}, V_{Pmicro} = 0.3 cm^3 g^{-1}).[3] This is in agreement with comparable sizes of ADC and Fum linkers. It is worth noting that the surface area of Ce-HHU-1 is larger than that we previously obtained for Zr-HHU-1 (570 m^2 g^{-1}).[12] This could be explained by the fact that Ce-HHU-1 is synthesized in water without modulator, which could have enabled a better evacuation of its pores, whereas Zr-HHU-1 was synthesized in DMF and using acetic acid as crystallization modulator.

The water sorption isotherm obtained at 20 °C exhibits a type I isotherm similar to that of Zr-HHU-1 (Fig. 5),[12] revealing

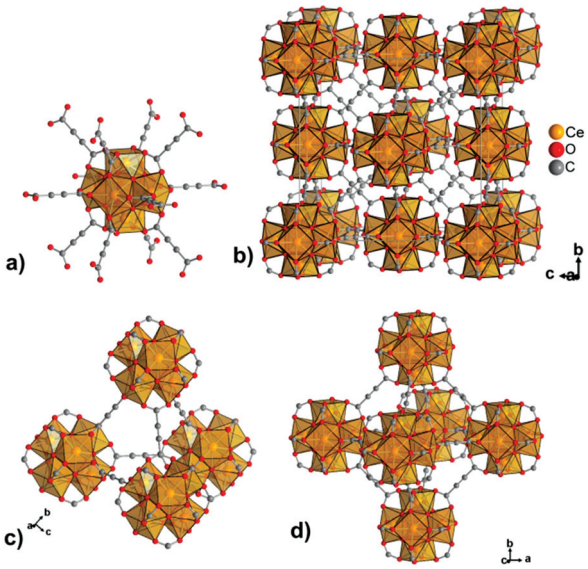

Fig. 3 (a) Secondary building unit of $\{Ce_6O_4(OH)_4\}$ with the twelve surrounding and connecting acetylenedicarboxylate linkers and the edge-sharing square-antiprismatic Ce_6O_8 polyhedra (b) fcc packing diagram of the **fcu** network in Ce-HHU-1 (c) tetrahedral cage (d) octahedral cage.

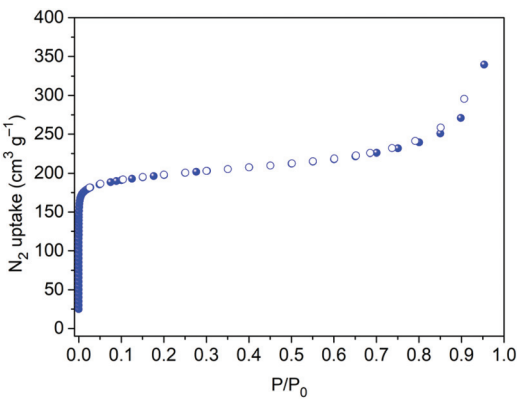

Fig. 4 Nitrogen sorption isotherm for Ce-HHU-1 at 77 K (filled symbols: adsorption; empty symbols: desorption).

the high hydrophilicity of the material. This is in agreement with their analogous compositions and structures. The water uptake capacity of about 208 mg g^{-1} is in agreement with the micropore volume. It is worth noting that the crystallinity of Ce-HHU-1 was maintained after the water sorption experiment with only small loss in the surface area (793 m^2 g^{-1} before and 731 m^2 g^{-1} after water sorption). The high hydrophilicity and water uptake capacity of Ce-HHU-1 indicate that this material can be applied for dehumidification/desiccation purpose.[23]

The CO_2 sorption isotherms of Ce-HHU-1 obtained at 273 and 293 K respectively (Fig. 6a), exhibit a type I shape which is in agreement with its microporous nature. The CO_2 uptake capacity at 1 bar amounts to 3.2 and 2.5 mmol g^{-1} at 273 K and 293 K respectively. We note that the CO_2 uptake capacity

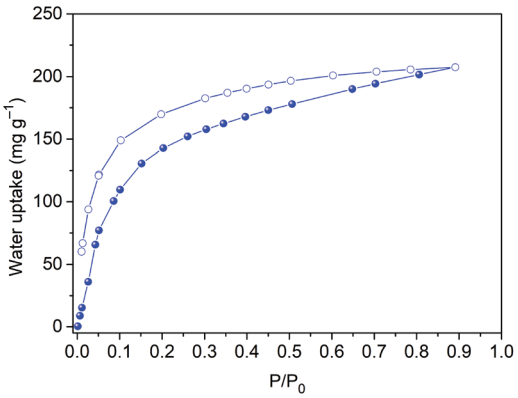

Fig. 5 Water vapor sorption isotherm for Ce-HHU-1 at 20 °C (filled symbols: adsorption; empty symbols: desorption).

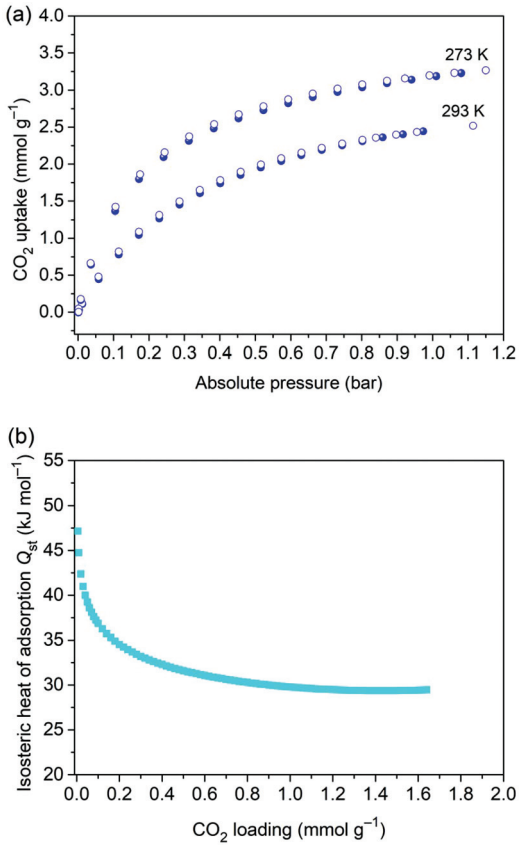

Fig. 6 (a) CO_2 sorption isotherms at 273 K and 293 K. (b) Plot of isosteric heat of CO_2 adsorption with loading for Ce-HHU-1 (filled symbols: adsorption; empty symbols: desorption).

of Ce-HHU-1 is higher than most reports of CO_2 adsorption in Ce(IV)-based MOFs (see Table S1 in ESI†). Its uptake is also comparable with those of Zr-UiO-66 (2.3 mmol g^{-1}), Zr-UiO-NH$_2$ (2.6 mmol g^{-1}) and Zr-UiO-67 (2.51 mmol g^{-1}) under ambient (293 K, 1 bar) conditions.[24,25] Thus, Ce-HHU-1 has an interesting CO_2 adsorption capability and can therefore be considered a prospective material for CO_2 capture and storage.

The isosteric heat of absorption Q_{st} calculated using the Clausius Clapeyron equation from isotherms obtained at 273 K and 293 K is plotted in Fig. 6b (see calculation details in ESI†). The zero coverage heat of adsorption Q_{st}^0 of about 47 kJ mol^{-1} is higher than that reported for UiO-66 (28 kJ mol^{-1}), zirconium and hafnium fumarate (19–29 kJ mol^{-1}) for example.[26] Such a high heat of adsorption was previously attributed to the synergistic effect of pore size reduction, μ_3-OH groups on metal-clusters and most especially to the –C≡C– triple-bond in the framework.[12]

Adsorption of bromine and iodine vapors

The capital importance of elemental halogens (mostly Cl_2 and Br_2) in industry contrasts with their hazardous nature due to their high toxicity, volatility and corrosiveness.[27] It is of great importance to find solid materials that can capture bromine and chlorine in case of spillage and leakage or for routine safety of workers and installations in halogen production units.[28] Many studies highlight the negative impact of bromine on human health and its contribution to ozone layer depletion.[29]

The presence of the alkyne function within the framework of Ce-HHU-1 prompted us to investigate its adsorption properties towards halogen vapors. When placed in a closed vessel with a small amount of bromine, 30 mg of Ce-HHU-1 completely adsorb and clean up the vessel space from the brownish smog, as well as empty the bromine container within few days (Fig. 7). Surprisingly, the material is transformed into a new highly crystalline and light yellow product showing no trace of the red-brownish color of Br_2 (Fig. 7). The product Ce-HHU-1-Br_2 has a completely different structure as seen from the PXRD patterns (Fig. 8). This indicates that Br_2 is completely irreversibly chemisorbed by Ce-HHU-1. The liquid NMR analysis reveals that the new adduct contains the 2,3-dibromofumarate linker (see Fig. S10 in ESI†). This indicates that the triple-bond of ADC in Ce-HHU-1 undergoes a solid state dibromination leading to a dibromoalkene-based coordination polymer/complex in a microcrystalline-to-microcrystalline fashion. The new compound is soluble in water and other organic solvents, suggesting that the $Ce_6O_4(OH)_4$ cluster is also altered by reacting with Br_2. However, the determination of the

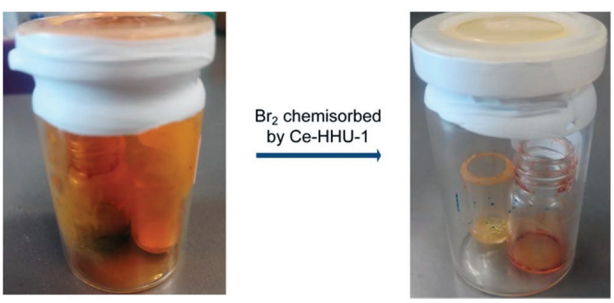

Fig. 7 Photographs of the set-up for bromine vapor adsorption with Ce-HHU-1. A complete clean-up of the vessel from bromine is observed after some days.

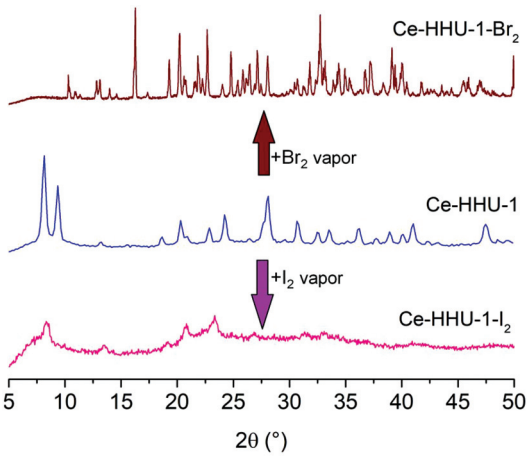

Fig. 8 Powder X-ray diffractograms of Ce-HHU-1, compared to adducts obtained after iodine and bromine vapor adsorption.

exact structure of Ce-HHU-1-Br_2 is out of the scope of this work. We anticipate that a similar chemisorption with Ce-HHU-1 could also take place with chlorine vapor.

Ce-HHU-1 has high ability for fixation of bromine vapor and can therefore be used in filtration sets like gas masks, or can be applied to clean polluted air from toxic bromine gas. We note that scarce reports are found where a solid material like Ce-HHU-1 can chemisorb bromine vapor and clean spaces polluted by this toxic vapor.

The adsorption of molecular iodine (I_2) vapor was also conducted gravimetrically with an activated sample of Ce-HHU-1 at room temperature. The adsorption of I_2 was evidenced by a progressive color change of Ce-HHU-1 from yellow to brown (Fig. S11, ESI†). The curve of iodine uptake with time (Fig. 9) shows that Ce-HHU-1 has an iodine adsorption capacity of about 0.8 g g^{-1}. In the Raman spectrum of iodine loaded sample I_2@Ce-HHU-1 (Fig. S13, ESI†), a decrease in intensity of the band related to the triple bond at 2225 cm^{-1} is observed, as well as the increase of the band at 1600 cm^{-1} suggesting a partial transformation of some triple-bonds to double-bonds. The ^{13}C NMR spectrum of the digested washed sample post-iodine sorption (Fig. S12, ESI†) has three peaks at 167, 91, and

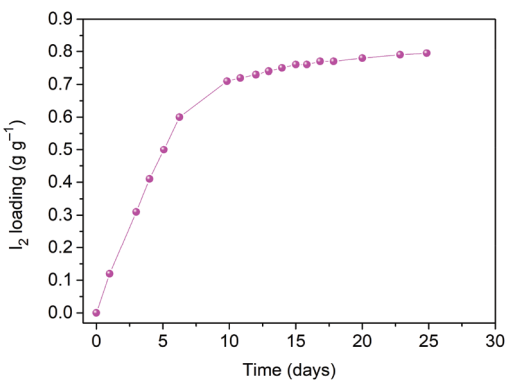

Fig. 9 Plot of iodine vapor adsorption with time for Ce-HHU-1.

85 ppm corresponding to the carbon of the carboxylate, the iodine substituted olefinic carbon and of the triple-bond respectively. In addition, new distinct bands at 1000, 800, 717, 522 cm^{-1} appear in the Raman spectrum (Fig. S13, ESI†) which correspond to the formation of new bonds, notably the =C–I bond. It is worth noting that the new bands remain after full I_2 desorption by washing over one week. The washing consisted in stirring I_2@Ce-HHU-1 in ethanol for a week, changing the solvent twice each day. The aforementioned observations indicate that iodine is both physisorbed and chemisorbed in Ce-HHU-1. The chemisorption consists of a diiodination of some of the –C≡C– triple bonds of the ADC linker to a diiodofumarate linker. The PXRD pattern of the iodine-loaded sample (Fig. 8) shows that the framework collapses upon adsorption of iodine to a poorly crystalline phase. The adsorption of I_2 in Ce-HHU-1, therefore results in the solid state diiodination of some of the triple-bonds in the framework.

The Raman spectrum of I_2@Ce-HHU-1 presents also very strong bands at 169 and 111 cm^{-1} (Fig. S13, ESI†). These bands are characteristics for I_5^- and I_3^- polyiodides respectively.[30] Interestingly, these bands persist in the thoroughly washed sample, although slightly shifted (159 and 110 cm^{-1} for I_5^- and I_3^- respectively) with reduced intensity. This indicates the formation of stable polyiodide ions from the interaction of I_2 with covalently bonded I (=C–I···I_2). The iodine adsorption and storage capacity of Ce-HHU-1 demonstrates the potential application of this material for radioactive I_2 sequestration.

Conclusions

This work establishes the potential of the acetylenedicarboxylate linker in the construction of permanently porous metal–organic frameworks. The new UiO-type MOF (Ce-HHU-1) based on acetylenedicarboxylate linker and Ce(IV) cations has successfully been synthesized and structurally characterized by Rietveld refinement. Its permanent microporosity has been demonstrated by nitrogen sorption experiment, while its high hydrophilicity is evidenced from the water sorption isotherm of type I. This material features a high isosteric heat of CO_2 adsorption attributable to the effect of the triple-bond. Ce-HHU-1 is a good halogen vapor adsorbent, of which bromine undergoes a complete chemical fixation to a new crystalline material *via* halogenation of the triple-bond. The later property makes Ce-HHU-1 a potential material for application in the capture of hazardous halogen vapors.

Conflicts of interest

There are no conflicts to declare.

Acknowledgements

We thank the German Academic Exchange Service (DAAD) for funding to TJMMN through grant no. 57214225 and the

Federal Ministry of Education and Research (BMBF) for project Optimat, grant no. 03SF0492C. We also thank Mr. Bastian Moll for conducting the Raman spectroscopy measurements.

References

1 (*a*) S. Smolders, K. A. Lomachenko, B. Bueken, A. Struyf, A. L. Bugaev, C. Atzori, N. Stock, C. Lamberti, M. B. J. Roeffaers and D. E. De Vos, *ChemPhysChem*, 2018, **19**, 373–378; (*b*) X.-J. Hong, C.-L. Song, Y. Yang, H.-C. Tan, G.-H. Li, Y.-P. Cai and H. Wang, *ACS Nano*, 2019, **13**, 1923–1931.

2 X.-P. Wu, L. Gagliardi and D. G. Truhlar, *J. Am. Chem. Soc.*, 2018, **140**, 7904–7912.

3 M. Lammert, M. T. Wharmby, S. Smolders, B. Bueken, A. Lieb, K. A. Lomachenko, D. De Vos and N. Stock, *Chem. Commun.*, 2015, **51**, 12578–12581.

4 M. Lammert, C. Glißmann, H. Reinsch and N. Stock, *Cryst. Growth Des.*, 2017, **17**, 1125–1131.

5 S. Smolders, A. Struyf, H. Reinsch, B. Bueken, T. Rhauderwiek, L. Mintrop, P. Kurz, N. Stock and D. E. De Vos, *Chem. Commun.*, 2018, **54**, 876–879.

6 (*a*) R. Dalapati, B. Sakthivel, A. Dhakshinamoorthy, A. Buragohain, A. Bhunia, C. Janiak and S. Biswas, *CrystEngComm*, 2016, **18**, 7855–7864; (*b*) K. A. Lomachenko, J. Jacobsen, A. L. Bugaev, C. Atzori, F. Bonino, S. Bordiga, N. Stock and C. Lamberti, *J. Am. Chem. Soc.*, 2018, **140**, 17379–17383.

7 J. H. Cavka, S. Jakobsen, U. Olsbye, N. Guillou, C. Lamberti, S. Bordiga and K. P. Lillerud, *J. Am. Chem. Soc.*, 2008, **130**, 13850–13851.

8 C. Serre, J. Marrot and G. Férey, *Inorg. Chem.*, 2005, **44**, 654–657.

9 D. J. Tranchemontagne, J. R. Hunt and O. M. Yaghi, *Tetrahedron*, 2008, **64**, 8553–8557.

10 V. K. Gramm, A. Schuy, M. Suta, C. Wickleder, C. Sternemann and U. Ruschewitz, *Z. Anorg. Allg. Chem.*, 2018, **644**, 127–135.

11 A. Michaelides and S. Skoulika, *Cryst. Growth Des.*, 2005, **5**, 529–533.

12 (*a*) T. J. Matemb Ma Ntep, H. Reinsch, B. Moll, E. Hastürk, S. Gökpinar, H. Breitzke, C. Schlüsener, L. Schmolke, G. Buntkowsky and C. Janiak, *Chem. – Eur. J.*, 2018, **24**, 14048–14053; (*b*) T. J. Matemb Ma Ntep, H. Reinsch, C. Schlüsener, A. Goldman, H. Breitzke, B. Moll, L. Schmolke, G. Buntkowsky and C. Janiak, *Inorg. Chem.*, 2019, **58**, 10965–10973.

13 (*a*) R. J. Marshall, S. L. Griffin, C. Wilson and R. S. Forgan, *J. Am. Chem. Soc.*, 2015, **137**, 9527–9530; (*b*) R. J. Marshall, S. L. Griffin, C. Wilson and R. S. Forgan, *Chem. – Eur. J.*, 2016, **22**, 4870–4877.

14 Z. Yan, Y. Yuan, Y. Tian, D. Zhang and G. Zhu, *Angew. Chem., Int. Ed.*, 2015, **54**, 12733–12737.

15 (*a*) R. D'Amato, A. Donnadio, M. Carta, C. Sangregorio, D. Tiana, R. Vivani, M. Taddei and F. Costantino, *ACS Sustainable Chem. Eng.*, 2019, **7**, 394–402; (*b*) J. Jacobsen, B. Achenbach, H. Reinsch, S. Smolders, F.-D. Lange, G. Friedrichs, D. De Vos and N. Stock, *Dalton Trans.*, 2019, **48**, 8433–8441; (*c*) S. Waitschat, D. Fröhlich, H. Reinsch, H. Terraschke, K. A. Lomachenko, C. Lamberti, H. Kummer, T. Helling, M. Baumgartner, S. Henninger and N. Stock, *Dalton Trans.*, 2018, **47**, 1062–1070.

16 (*a*) H. Reinsch, *Eur. J. Inorg. Chem.*, 2016, 4290–4299; (*b*) S. Wang and C. Serre, *ACS Sustainable Chem. Eng.*, 2019, **7**, 11911–11927.

17 R. Shannon, *Acta Crystallogr., Sect. A: Cryst. Phys., Diffr., Theor. Gen. Crystallogr.*, 1976, **32**, 751–767.

18 (*a*) H. Billetter, F. Hohn, I. Pantenburg and U. Ruschewitz, *Acta Crystallogr., Sect. C: Cryst. Struct. Commun.*, 2003, **59**, 130–131; (*b*) I. Pantenburg and U. Ruschewitz, *Z. Anorg. Allg. Chem.*, 2002, **628**, 1697–1702; (*c*) U. Ruschewitz and I. Pantenburg, *Acta Crystallogr., Sect. C: Cryst. Struct. Commun.*, 2002, **58**, 483–484; (*d*) I. Stein and U. Ruschewitz, *Z. Anorg. Allg. Chem.*, 2010, **636**, 400–404; (*e*) A. Schuy, I. Stein and U. Ruschewitz, *Z. Anorg. Allg. Chem.*, 2010, **636**, 1026–1031; (*f*) S. Busch, I. Stein and U. Ruschewitz, *Z. Anorg. Allg. Chem.*, 2012, **638**, 2098–2101.

19 F. Hohn, I. Pantenburg and U. Ruschewitz, *Chem. – Eur. J.*, 2002, **8**, 4536–4541.

20 G. C. Shearer, S. Chavan, J. Ethiraj, J. G. Vitillo, S. Svelle, U. Olsbye, C. Lamberti, S. Bordiga and K. P. Lillerud, *Chem. Mater.*, 2014, **26**, 4068–4071.

21 Coelho Software, *Topas Academics 4.2*, 2007.

22 M. Thommes, K. Kaneko, A. V. Neimark, J. P. Olivier, F. Rodriguez-Reinoso, J. Rouquerol and K. S. W. Sing, *Pure Appl. Chem.*, 2015, **87**, 1051–1069.

23 (*a*) P. Guo, A. G. Wong-Foy and A. J. Matzger, *Langmuir*, 2014, **30**, 1921–1925; (*b*) P. Kenfack Tsobnang, E. Hastürk, D. Fröhlich, E. Wenger, P. Durand, J. Lambi Ngolui, C. Lecomte and C. Janiak, *Cryst. Growth Des.*, 2019, **19**, 2869–2880.

24 Y. Lin, C. Kong, Q. Zhang and L. Chen, *Adv. Energy Mater.*, 2017, **7**, 1601296.

25 P. Xydias, I. Spanopoulos, E. Klontzas, G. E. Froudakis and P. N. Trikalitis, *Inorg. Chem.*, 2014, **53**, 679–681.

26 (*a*) Z. Hu, Y. Peng, Z. Kang, Y. Qian and D. Zhao, *Inorg. Chem.*, 2015, **54**, 4862–4868; (*b*) Z. Hu, I. Castano, S. Wang, Y. Wang, Y. Peng, Y. Qian, C. Chi, X. Wang and D. Zhao, *Cryst. Growth Des.*, 2016, **16**, 2295–2301.

27 P. Coleman, R. Mascarenhas and P. Rumsby, *A Review of the Toxicity and Environmental Behaviour of Bromine in Air*, Environment Agency, Rio House, Waterside Drive, Aztec West, Almondsbury, Bristol, BS32 4UD, 2005.

28 R. C. Liimatainen and W. J. Mecham, *J. Air Pollut. Control Assoc.*, 1956, **6**, 17–49.

29 (*a*) B. J. Finlayson-Pitts, F. E. Livingston and H. N. Berko, *Nature*, 1990, **343**, 623–625; (*b*) G. Lammel, A. Röhrl and H. Schreiber, *Environ. Sci. Pollut. Res.*, 2002, **9**, 397–404.

30 (*a*) I. D. Yushina, B. A. Kolesovb and E. V. Bartashevicha, *New J. Chem.*, 2015, **39**, 6163–6170; (*b*) P. Deplano, J. R. Ferraro, M. L. Mercuri and E. F. Trogu, *Coord. Chem. Rev.*, 1999, **188**, 71–95; (*c*) E. M. Nour, L. H. Chen and J. Laane, *J. Phys. Chem.*, 1986, **90**, 2841–2846.